

Supporting Information

Biocarbon-templated synthesis of porous Ni-Co-O nanocomposites for room-temperature NH₃ sensors

Huan Liu^a, He Lv^a, Kan Kan^{b,c}, Yang Liu^a, Weijun Zhang^c, Yang Wang^a, Muhammad Ikram^a, Lijuan Du^d, Keying Shi^{a,*}, Hai-tao Yu^{a,*}

^a Key Laboratory of Functional Inorganic Material Chemistry (Ministry of Education)
and School of Chemistry and Material Science, Heilongjiang University, Harbin, 150080,
China

^b Daqing Branch, Heilongjiang Academy of Sciences, Daqing 163319, China.

^c Institute of Advanced Technology, Heilongjiang Academy of Science, Harbin, 150080,
China

^d Harbin Normal University, Harbin 150025, China

*** Corresponding author.**

E-mail: yuhaitao@hlju.edu.cn (Prof. H.-T. Yu); shikeying2008@163.com (Prof. K. Y. Shi). Fax: +86 451 8667 3647; Tel: +86 451 8660 9141

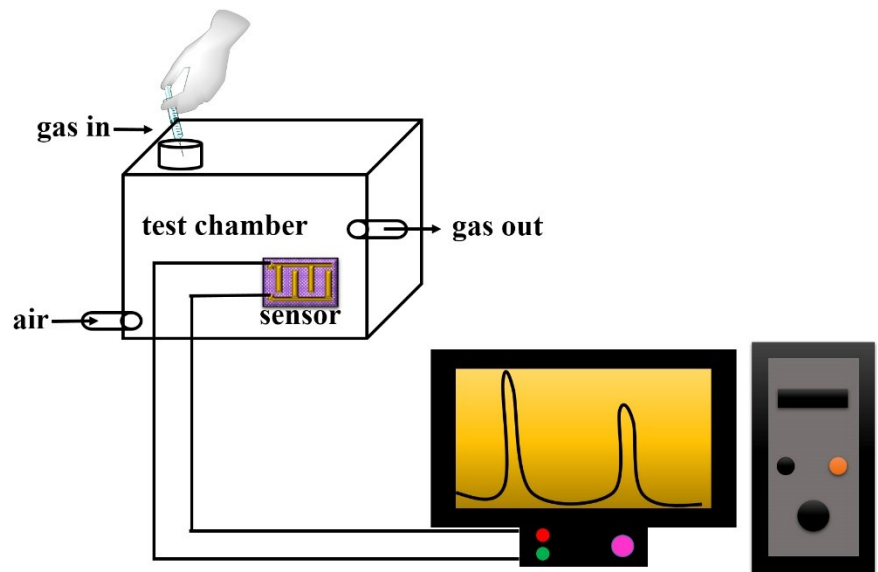


Fig. S1. Gas-sensing tests of thin-film sensors.

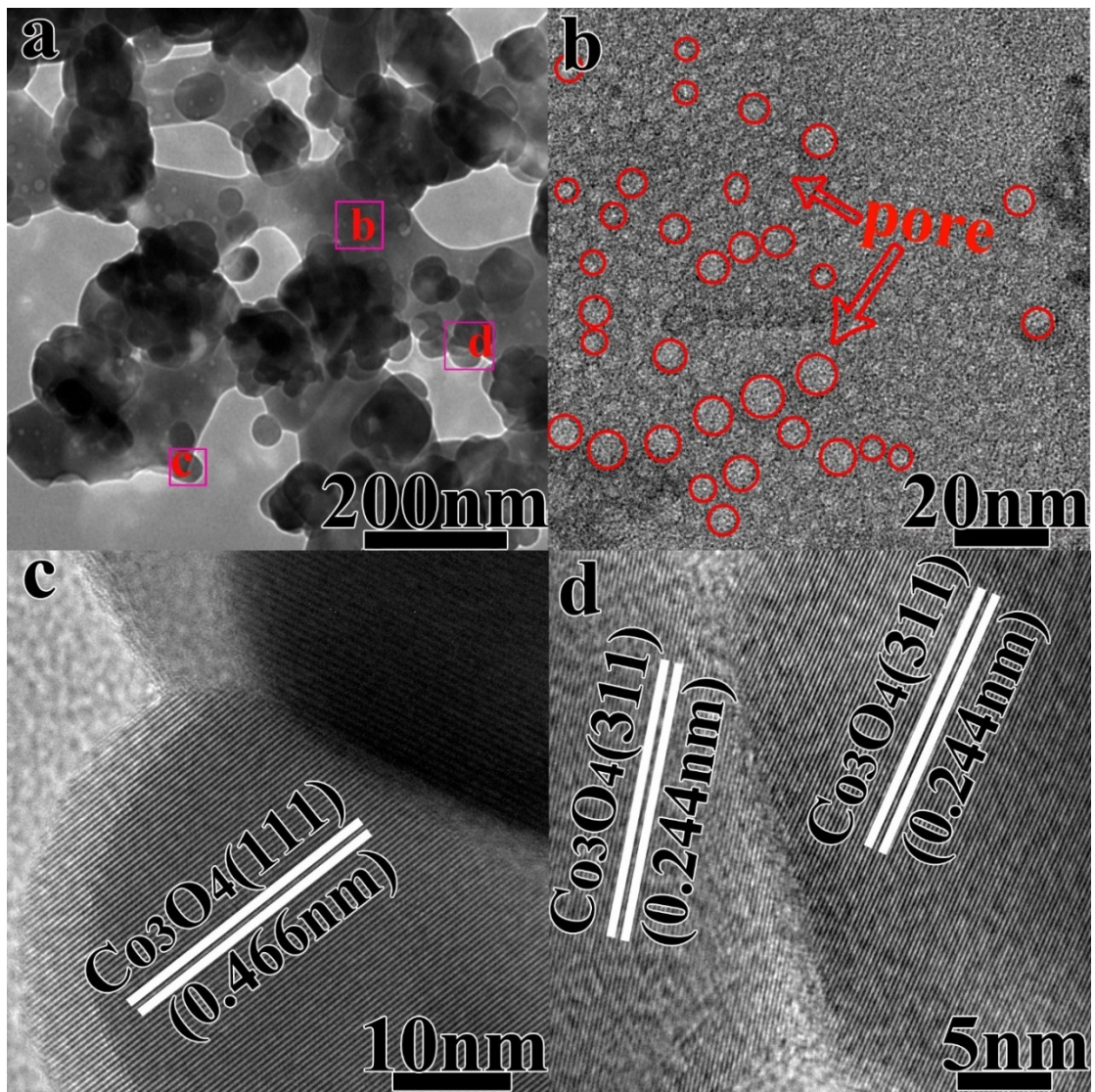


Fig. S2. TEM/HRTEM images of **C1**: (a) Low magnification image, (b, c) Enlarged TEM images, and (d) HRTEM image.

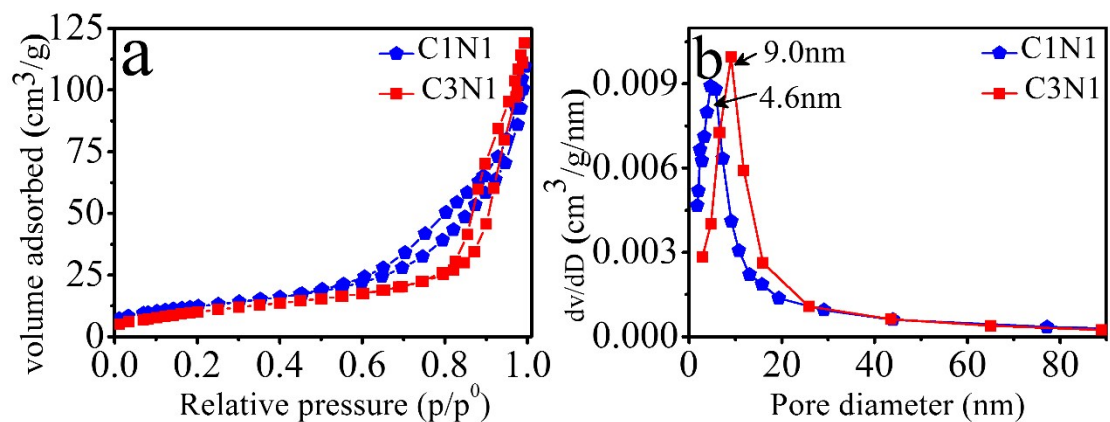


Fig. S3. N₂ adsorption-desorption isotherms and pore size distributions of **C1N1** and **C3N1**.

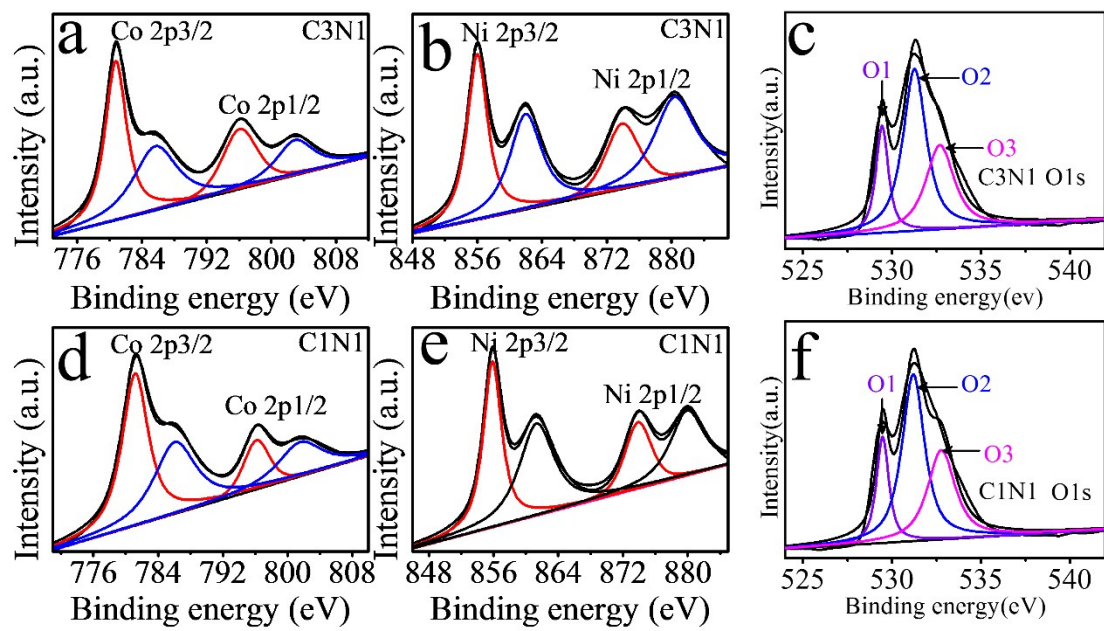


Fig. S4. XPS spectra: (a) Co 2p, (b) Ni 2p, and (c) O 1s of **C3N1** and (d) Co 2p, (e) Ni 2p, and (f) O 1s of **C1N1**.

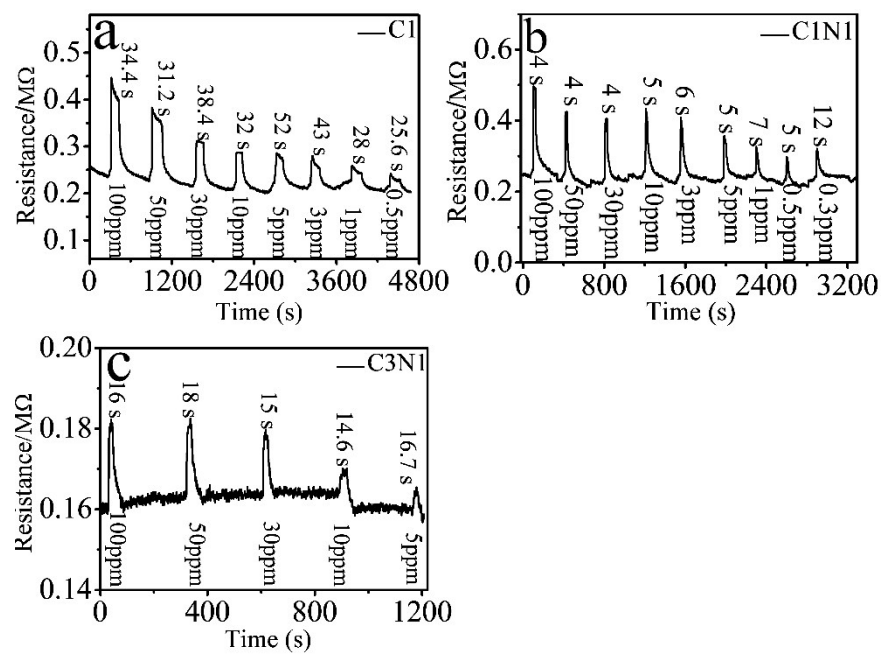


Fig. S5. Dynamical response-recovery curves of (a) C1, (b) C1N1, and (c) C3N1 towards NH_3 at RT.

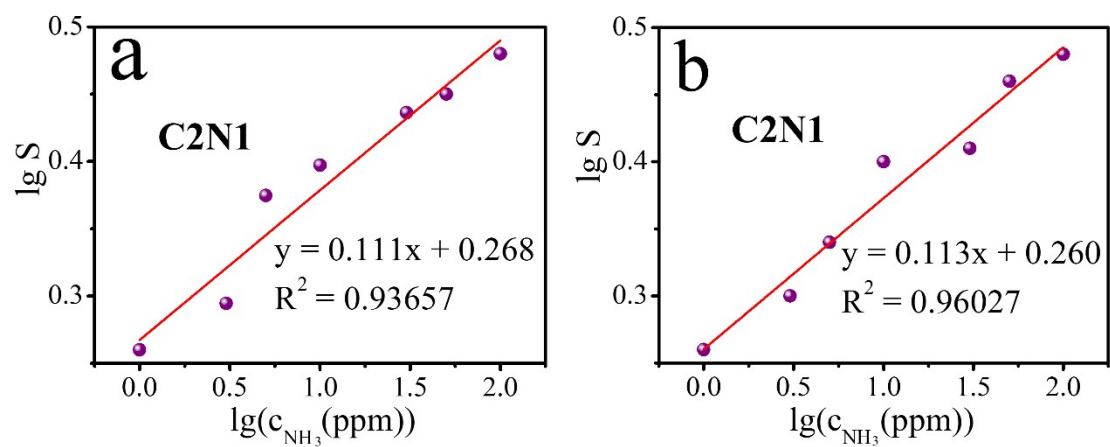


Fig. S6 Fitted NH₃ concentration-dependent response of **C2N1**.

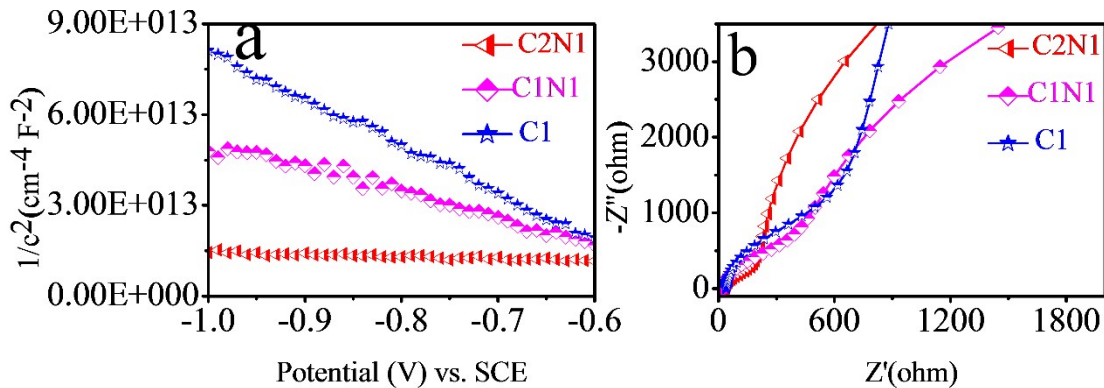


Fig. S7. (a) Mott-Schottky plots of the **C2N1**, **C1N1**, and **C1** electrodes in 2 mol L $^{-1}$ KOH electrolyte measured at a frequency of 1 kHz. (b) Nyquist plots of **C2N1**, **C1N1**, and **C1** measured in the frequency range of 0.01 Hz to 100 kHz

The carrier densities of **C2N1**, **C1**, and **C1N1** were measured by the Mott-Schottky method. In Fig. S7a, the Mott-Schottky curves of the three samples show a negative slope, which means that they are *p*-type semiconducting materials. Their carrier densities can be calculated using the equation [1]

$$Nd = -\frac{2}{\epsilon_0 e_0 \epsilon} \left(\frac{d(1/c^2)}{dv} \right)^{-1} \quad (\text{S1})$$

where e^0 is the fundamental charge constant ($e^0 = 1.6 \times 10^{-19}$ C), ϵ^0 is the permittivity of vacuum 8.85×10^{-14} F cm $^{-1}$, ϵ is the relative permittivity of Co₃O₄ (12.9) [2], $(d(1/c^2)/dv)^{-1}$ is the slope of the Mott-Schottky plots. In addition, the electrochemical impedance spectroscopy (EIS) were measured to investigate the charge transfer of the gas sensor materials. In Fig. S8b, the impedance spectra of **C2N1**, **C1N1**, and **C1** exhibit a similar semicircle followed by a slope line and possess a similar appropriate equivalent circuit model (see the inset in Fig. 7b). The obtained impedance parameters are shown in Table S5, in which $R\Omega$ can be attributed to the resistance of the electrolyte, separator, and electrode, R_{ct} is the charge transfer resistance at the active interface of material, and CPE is constant phase angle element, involving double layer capacitance.

Chem. A, 2014, **2**, 4961-4969.

2 S. Thota, A. Kumar and J. Kumar, *Optical, Mater. Sci. Eng., B*, 2009, **164**, 30-37.

Table S1 Calculated $2p$ binding energies (in eV) of different spin orbital splitting states from the XPS spectra.

Samples	Co 2p _{3/2}	Co 2p _{1/2}	Ni 2p _{3/2}	Ni 2p _{1/2}
C1	779.8 (37.12%)	795.70 (19.07%)	/	/
C1N1	781.16 (41.91%)	796.16 (11.29%)	855.87 (30.88%)	873.88 (15.01%)
C2N1	779.53 (35.00%)	795.53 (14.69%)	853.3 (31.32%)	871.1 (18.33%)
C3N1	780.77 (36.70%)	796.10 (19.04%)	856.01 (29.62%)	873.92 (15.96%)

Table S2 O 1s peak positions (in eV) and calculated intergral peak areas (%) for the XPS spectra. The O(1), O(2), and O(3) refer to the lattice oxygen, defect oxygen, and oxygen in the adsorbed H₂O, respectively.

Sample	Oxygen species	Peak Position	Peak area
C1	O(1)	530.5	22.8
	O(2)	531.2	41.3
	O(3)	532.1	36.9
C1N1	O(1)	529.5	17.5
	O(2)	531.2	50.3
	O(3)	532.8	32.7
C2N1	O(1)	530.0	10.8
	O(2)	531.5	56.8
	O(3)	534.3	32.4
C3N1	O(1)	529.5	17.7
	O(2)	531.3	49.7
	O(3)	532.7	32.0

Table S3 Measured response dependence on NH₃ concentration (ppm) at room temperature.

Concentration	C1	C1N1	C2N1	C3N1
100	1.90	1.89	3.00	1.15
50	1.70	1.66	2.90	1.12
30	1.45	1.69	2.70	1.10
10	1.39	1.69	2.50	1.00
5	1.40	1.64	2.20	1.00
3	1.34	1.47	1.90	/
1	1.17	1.30	1.80	/
0.5	1.19	1.26	1.60	/
0.3	/	1.32	1.40	/
0.1	/	1.10	1.41	/
0.05	/	1.10	1.39	/

Table S4 Dependence of response time on NH₃ concentration at room temperature.

Concentration	C1	C1N1	C2N1	C3N1
100	34.4	4.0	3.0	16.0
50	31.2	4.0	4.0	18.0
30	38.4	4.0	4.2	15.0
10	32.0	5.0	5.0	14.6
5	52.0	6.0	6.0	16.7
3	43.0	5.0	8.0	/
1	28.0	7.0	9.0	/
0.5	25.6	5.0	12.0	/
0.3	/	12.0	15.0	/
0.1	/	/	16.0	/
0.05	/	/	19.0	/

Table S5 Comparison of the sensing performances of our proposed NH₃ sensor with those reported in the literature

Materials	Concentration (ppm)	Temperature (°C)	Response (R_g/R_a)	Detection limit (ppm)	References
Ni-Co-O nanocomposites	100	RT	3	0.05	This work
Co ₃ O ₄ nanonetworks	100	RT	2.46	0.5	[1]
Co ₃ O ₄ dendritic	200	110	1.63	-	[2]
Co ₃ O ₄ nanowire-like networks	100	300	<1.5	10	[3]
CuO nanowires	100	250	1.6	-	[4]
Cr/CuO	100	RT	0.9 ($\Delta R/R_a$)	-	[5]
Cu ₂ O nanorods/rGO	100	RT	1.77	-	[6]
SnO ₂ -SnS ₂ hybirds	100	RT	≈ 1.9	10	[7]
CuO superstructures	100	RT	≈ 0.75	-	[8]

RT: room temperature.

Table S6 Calculated carrier concentrations (N_d , cm^{-3}) and fitted impedance parameters R_Ω (in Ω), R_{ct} (in Ω), and CPE (in F cm^{-2}) in equivalent circuit models.

Samples	R_Ω	R_{ct}	CPE	N_d
C1	38.83	249.92	3.11×10^{-5}	6.21×10^{17}
C2N1	11.04	77.98	1.07×10^{-3}	1.57×10^{18}
C1N1	22.56	196.82	8.09×10^{-3}	1.16×10^{18}

References:

1. B. Wu, L. Wang, H. Wu, K. Kan, G. Zhang, Y. Xie, Y. Tian, L. Li and K. Shi, *Microporous Mesoporous Mater.*, 2016, **225**, 154-163.
2. X.X. Yu, X.S. Liu, M.Z. Wu, Z.Q. Sun and X.S. Chen, *Chin. J. Chem. Phys.*, 2014, **27**, 99-102.
3. S. Yi, S. Tian, D. Zeng, K. Xu, X. Peng, H. Wang, S. Zhang and C. Xie, *Sens. Actuators, B*, 2014, **204**, 351-359.
4. F. Shao, F. Hernández-Ramírez, J.D. Prades, C. Fàbrega, T. Andreu and J.R. Morante, *Appl Surf Sci*, 2014, **311**, 177-181.
5. S. Bhuvaneshwari and N. Gopalakrishnan, *J. Alloys Compd.*, 2016, **654**, 202-208.
6. H. Meng, W. Yang, K. Ding, L. Feng and Y. Guan, *J. Mater. Chem. A*, 2015, **3**, 1174-1181.
7. K. Xu, N. Li, D. Zeng, S. Tian, S. Zhang, D. Hu and C. Xie, *ACS Appl. Mater. Interfaces*, 2015, **7**, 11359-11368.
8. S. Bhuvaneshwari and N. Gopalakrishnan, *J Colloid Interface Sci*, 2016, **480**, 76-84.